Interconversion of Brucite-like and Hydrotalcite-like Phases in Cobalt Hydroxide Compounds

Z. P. Xu and H. C. Zeng*

Department of Chemical Engineering, Faculty of Engineering, National University of Singapore, 10 Kent Ridge Crescent, Singapore 119260

Received June 10, 1998. Revised Manuscript Received October 6, 1998

Formation and interconversion of cobalt hydroxides have been investigated with XRD, FTIR, and compositional analysis. Effects of addition time, aging time, and preparative atmosphere on phase transformation and materials synthesis in ammoniacal solution have been systematically examined. A new precursor phase with hydrotalcite-like characteristics has been identified. While α-$Co(OH)_2$ is prepared with short-aging in nitrogen atmosphere, this divalent metal (Co^{2+}) hydrotalcite-like phase transforms into brucite-like β-$Co(OH)_2$ under prolonged aging in nitrogen. The β-$Co(OH)_2$ can be formed readily in air but later is converted into a new hydrotalcite-like phase which is stable and contains both Co^{2+} and Co^{3+} due to redox reactions. Interconversions among the four structural phases have been investigated and correlated.

Introduction

Transition-metal layered-hydroxide materials such as $Ni(OH)_2$ and $Co(OH)_2$ have received increasing attention in recent years, due to their many important technological applications.[1−11] In their simplest structure, brucite-like phases form a close-packed array in which a divalent metal cation is located in an octahedral site generated by six hydroxyl oxygen atoms. These two-dimensional metal−hydroxyl sheets stack via hydrogen bonding to form a three-dimensional structure.[1] When some divalent cations are replaced by trivalent cations, anions in solution will be incorporated into the interlayer space to balance the extra positive charge carried by the trivalent ions. This intercalation process leads to formation of hydrotalcite(HT)-like structures that are named after the natural mineral $Mg_6Al_2(OH)_{16}CO_3 \cdot 4H_2O$ (Mg−Al−HT),[12,13] in which both Mg^{2+} and Al^{3+} are located in brucite ($Mg(OH)_2$) type sheets while CO_3^{2-} anions occupy the intersheet space to balance extra positive charges carried by trivalent Al^{3+} cations (compared to divalent Mg^{2+}).[12,13] Other types of HT formation are also possible. For example, when some of the hydroxyl groups are missing from their positions in the brucite-like sheets, intercalation of anions also occurs to restore charge neutrality.[11] Although no starting trivalent cations are required, resultant compounds produced in this way also have large interlayer spacings due to the anion occupation in the inter-brucite-like sheets.[11]

One important area in layered-hydroxide material research is phase transformation during compound synthesis. Despite great emphasis on materials synthesis and characterization, research to understand phase transformation phenomenon is relatively lacking. As an example, cobalt hydroxides, which are important electrode and catalytic materials, have been prepared by precipitation with liquid ammonia and by electrosynthetic routes using the cathodic reduction of cobalt nitrate solution.[2,6,10,11,14] Two polymorphic forms, α- and β-$Co(OH)_2$, have been found. The first one is isostructural with hydrotalcite-like compounds while the second is brucite-like. The HT-like phase (α-$Co(OH)_2$) converts spontaneously into more stable β-$Co(OH)_2$ in alkaline medium, i.e., forming brucite-like compounds.[2,6,10,11] Concerning the exact mechanism of intercalation of anion species in the α-phase hydrotalcite, a number of speculative models have been proposed.[1,2,6−8] Among them, two prominent models, "hydroxyl vacancies" and "mixed valent state (II and III)" have shown some validity.[2,6] In particular, the hydroxyl vacancies model has been very recently confirmed.[11] However, a more detailed picture of the interconversion between the α- and β-phases is largely unknown, especially when related to conversion conditions, such as the synthetic

* Corresponding author Tel: +65 874 2896. Fax: +65 779 1936. E-mail: chezhc@nus.edu.sg.

(1) Bish, D. L.; Livingstone, A. *Miner. Mag.* **1981**, *44*, 339.
(2) Faure, C.; Delmas, C.; Fousassier, M. *J. Power Sources* **1991**, *35*, 279.
(3) Faure, C.; Delmas, C.; Fousassier, M.; Willmann P. *J. Power Sources* **1991**, *35*, 249.
(4) Faure, C.; Delmas, C.; Willmann P. *J. Power Sources* **1991**, *35*, 263.
(5) Faure, C.; Borthomieu, Y.; Delmas, C.; Fousassier, M. *J. Power Sources* **1991**, *36*, 113.
(6) Kamath, P. V.; Vasanthacharya, N. Y. *J. Appl. Electrochem.* **1992**, *22*, 483.
(7) Rabu, P.; Angelov, S.; Legoll, P.; Belaiche, M.; Drillon, M. J. *Inorg. Chem.* **1993**, *32*, 2463.
(8) Benard, P.; Auffredic, J. P.; Louer, D. *Thermochem. Acta* **1994**, *232*, 65.
(9) Delahaya-Vidal, A.; Tekaia Ehlsissen, K.; Genin, P.; Figlarz, M. *Eur. J. Solid State Inorg. Chem.* **1994**, *31*, 823.
(10) Kamath, P. V.; Dixit, M.; Indira, L.; Shukla, A. K.; Kumar, V. G.; Munichandraiah, N. *J. Electrochem. Soc.* **1994**, *141*, 2956.
(11) Kamath, P. V.; Therese, G. H. A. *J. Solid State Chem.* **1997**, *128*, 38.
(12) Cavani, F.; Trifiro, F.; Vaccari, A. *Catal. Today* **1991**, *11*, No. 2, 173.
(13) Reichle, W. T. *Solid State Ionics* **1986**, *22*, 135.
(14) Dixit, M.; Subbanna, G. N.; Kamath, P. V. *J. Mater. Chem.* **1996**, *6*, 1429.

10.1021/cm980420b CCC: $18.00
Published on Web 12/24/1998

Table 1. Sample Nomenclature and Experimental Conditions

sample	atmosphere	addition time	aging time	sample	atmosphere	addition time	aging time
N00	nitrogen	15 s	15 s	NA01	nitrogen; air[a]	15 s	0.5 h; 2 h[b]
N01	nitrogen	15 s	5 min	NA02	nitrogen; air	5 min	0.5 h; 2 h
N02	nitrogen	15 s	2 h	NA03	nitrogen; air	10 min	0.5 h; 2 h
N03	nitrogen	15 s	4 h	NA04	nitrogen; air	35 min	0.5 h; 2 h
N04	nitrogen	15 s	6 h	NA05	nitrogen; air	75 min	0.5 h; 2 h
N05	nitrogen	15 s	8 h	NA06	nitrogen; air	1 min	1 h; 0 h
N06	nitrogen	15 s	2 h	NA07	nitrogen; air	1 min	1 h; 2 h
N07	nitrogen	10 min	2 h	NA08	nitrogen; air	1 min	1 h; 4 h
N08	nitrogen	20 min	2 h	NA09	nitrogen; air	1 min	1 h; 8 h
N09	nitrogen	30 min	2 h	NA10	nitrogen; air	1 min	1 h; 16 h
N10	nitrogen	60 min	2 h	NA11	nitrogen; air	1 min	1 h; 28 h
A00	air	15 s	15 s	NA12	nitrogen; air	1 min	1 h; 48 h
A01	air	15 s	15 min	NA13	nitrogen; air	1 min	1 h; 96 h
A02	air	15 s	30 min	NA14	nitrogen; air	10 min	20 h; 0 h
A03	air	15 s	45 min	NA15	nitrogen; air	10 min	20 h; 48 h
A04	air	15 s	60 min	NA16	nitrogen; air	10 min	20 h; 96 h
A05	air	4 min	3 min	AN01	air; nitrogen[c]	1 min	40 min; 0 h[d]
A06	air	4 min	2 h	AN02	air; nitrogen	1 min	40 min; 16 h
A07	air	4 min	4 h	AN03	air; nitrogen	1 min	40 min; 30 h
A08	air	4 min	8 h	AN04	air; nitrogen	1 min	40 min; 48 h
A09	air	4 min	16 h	AN05	air; nitrogen	1 min	16 h; 0 h
A10	air	4 min	24 h	AN06	air; nitrogen	1 min	16 h; 24 h
A11	air	4 min	48 h	AN07	air; nitrogen	1 min	16 h; 48 h
A12	air	15 s	2 h	AN08	air; nitrogen	1 min	16 h; 72 h
A13	air	9 min	2 h				
A14	air	22 min	2 h				
A15	air	42 min	2 h				

[a] Addition and the first part of aging in nitrogen; the second part of aging in air. [b] Time for the first part of aging in nitrogen; time for the second part of aging in air. [c] Addition and the first part of aging in air; the second part of aging in nitrogen. [d] Time for the first part of aging in air; time for the second part of aging in nitrogen.

atmosphere which provides additional chemical reactions and processing kinetics which involves time.

In this paper, we report a systematic investigation of the formation and interconversion of cobalt hydroxide compounds under various experimental conditions. A new precursor phase before the formation of α- and β-$Co(OH)_2$ has been found for the first time. Furthermore, in addition to the unstable hydrotalcite-like (α-) to brucite-like phase (β-) transition, a new conversion from the brucite-like (β-) to another stable hydrotalcite-like phase has also been revealed in the current work, which confirms the mixed valent state model.[6] The addition time of cation, aging time, and preparative atmosphere are important parameters in directing the interphase transformation. Understanding these controlling factors enables us to tailor-make cobalt layered hydroxides with a desired crystallographic structure and electronic configuration for the metal cations.

Experimental Section

Materials Preparation. Cobalt hydroxides were prepared using the precipitation method. Briefly, 20.0 mL of 1.0 M aqueous cobalt nitrate solution (Fluka, $Co(NO_3)_2{\cdot}6H_2O$, >99.0%) was added into 100.0 mL of 0.5 M ammoniacal solution in a three-necked round-bottom flask in a certain period of time (Table 1). The addition and precipitation were carried out under stirring and ambient control with either purified nitrogen [Soxal, O_2 < 2 vpm (volume per million)] or purified air (Soxal, $O_2 = 21 \pm 1\%$, H_2O < 2 vpm, and hydrocarbons < 5 vpm) bubbling through the solution at a rate of 40 mL/min at room temperature. In the former case (N_2), the ammoniacal solution was purged with nitrogen for 15−20 min to drive away dissolved oxygen before adding Co^{2+} cations. For short addition-time experiments (such as 15 s), the Co^{2+} solution was dumped rapidly from a funnel flask into the ammoniacal solution, while for the longer ones, the Co^{2+} was added dropwise with a constant time interval. The stirring and ambient control were continued during the aging of the precipitate for a desired length of time (Table 1), after which the precipitate was filtered and washed thoroughly with deionized water, followed by drying in a vacuum desiccator at room-temperature overnight. Three important preparative parameters were varied in the experiments: (i) addition time, (ii) aging time, and (iii) atmosphere used during the addition/aging. Final pH values of the filtrate were in the range of 8.5−8.2 depending on the addition/aging time of experiment. Table 1 reports synthetic conditions and nomenclature for each precipitate sample.

Material Characterization. Crystallographic information on the samples was investigated by powder X-ray diffraction (XRD) methods. Diffraction patterns of intensity versus 2θ were recorded with a Shimadzu XRD-6000 X-ray diffractometer with Cu Kα radiation (λ = 1.5418 Å) from 8° to 40° at a scanning speed of 3°/min. The interlayer spacing of the resultant layered hydroxides was determined from the diffraction peak positions/patterns with structural analysis software, and the average size of precipitate crystallites was estimated by using the Debye−Scherrer formula.[15] Chemical bonding information on metal−oxygen, hydroxyl, and intercalated functional groups (such as nitrate anions) were investigated with Fourier transform infrared spectroscopy (FTIR, Shimadzu FTIR-8101) using the potassium bromide (KBr) pellet technique. Each FTIR spectrum was collected after 100 scans with a resolution of 2 cm^{-1}.

The nitrogen and carbon content of the prepared samples was measured with elemental analysis (EA, Perkin-Elmer 2400 CHN analyzer), and the cobalt content was determined by thermogravimetric analysis (air-TGA, Shimadzu TGA-50) based on the end products Co_3O_4 at 600 °C and CoO at 950 °C. The trivalent cobalt content in some important precipitates (N01, N05, A05-A11, and AN07, Tables 1 and 4) was determined by a redox titration method. In this type of experiment, 10.00 mg of solid sample was dissolved in 20.0 mL of 1.0 M HCl solution with gentle heating. The produced Cl_2 gas was gradually purged with N_2 (60 mL/min) and sent to 50.0 mL of 0.01 M KI solution mixed with starch indicator. The resultant

(15) Cheetham, A. K.; Day, P. *Solid-State Chemistry: Techniques*; Clarendon Press: Oxford, 1987; p 79.

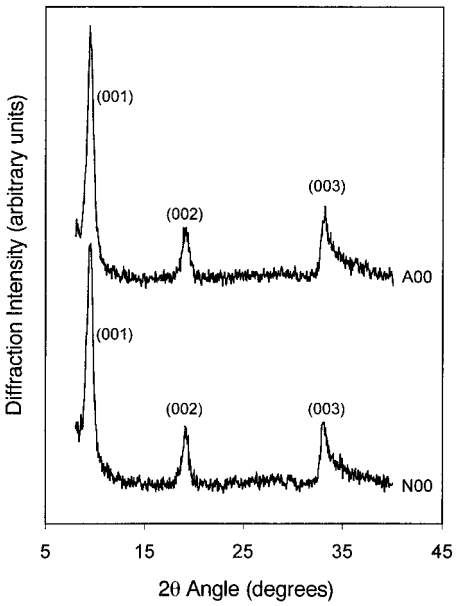

Figure 1. XRD patterns for the precursor samples N00 and A00.

Table 2. XRD Analysis Results for Samples with Different Crystallographic Phases

sample	phase[a]	interlayer space, Å	particle size, nm	layer number
N00	pre-HT	9.34	10.5	11
N01	HT(II)	8.09	8.0	10
N05	B(II)	4.66	60.0	130
AN08	HT(II,III)	7.98	12.0	15

[a] Pre-HT = pre-hydrotalcite-like phase; HT(II) = Co(II) hydrotalcite-like phase (i.e., α-$Co(OH)_2$); B(II) = Co(II) brucite-like phase [i.e., β-$Co(OH)_2$]; HT(II,III) = Co(II,III) hydrotalcite-like compound.

blue mixture was then titrated against a $Na_2S_2O_3$ solution (0.0100 M) until the blue disappeared.

Results and Discussion

Formation of Pre-Hydrotalcite-like Phase in either Nitrogen or Air. When the Co^{2+} is added rapidly into ammoniacal solution, a precipitate is formed instantaneously, as in the cases of N00 (prepared in nitrogen; see Table 1) and A00 (prepared in air; see Table 1). As shown in XRD patterns of Figure 1, the above two samples all show certain hydrotalcite-like characteristics, although *d*-values corresponding to successive diffraction by the basal planes do not agree well with each other, i.e., $d_{001} \approx 2d_{002}$ but $\neq 3d_{003}$ if the diffraction assignment for hydrotalcite-like structure (unit cell with three slabs) is used.[12,13,16] Nevertheless, structural analysis indicates that both samples have a large interbasal plane distance of 9.34 Å (d_{001}, unit cell with one slab; Table 2),[17] regardless of the type of atmosphere utilized. Due to fast nucleation/formation, the crystallite size for this pre-HT-like phase is only around 11 nm, according to the Debye−Scherrer method.[15] Since they have a large intersheet space, the structure of N00 and A00 samples is designated literally as a pre-hydrotalcite-like phase. The two IR spectra for N00 and A00 are also identical (Figure 2). In agreement with the structural assignment, absorption peaks at

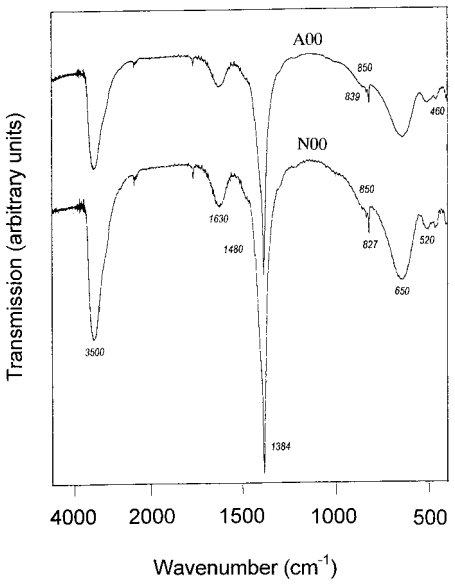

Figure 2. FTIR spectra for the precursor samples N00 and A00.

1384 and 839 cm^{-1} (ν_3 and ν_2 vibration modes of NO_3^- with D_{3h} symmetry) indicate that a large amount of NO_3^- anions are included. The broadening of the 1384 cm^{-1} peak and a low wavenumber for ν_2 mode (at 827 cm^{-1}) in both samples may suggest an interaction of NO_3^- anions with surroundings,[18−20] namely with intercalated water, hydroxyl groups, and cobalt cations in brucite-type layers.

Since the pre-HT-like phase is metastable and converts easily into other structures, the layer stacking in the pre-HT-like phase must be rather loose and defective, leading to a turbostratic structure.[21] This assignment is validated by the reflection peak shapes shown in Figure 1. For example, peak shapes of the reflections indexed as (001) and (002) are quite similar, whereas that of the (003) has a "saw-tooth" shape, a typical indication of turbostratic phases.[21] Furthermore, the ambient effect on precipitation synthesis is virtually negligible during the short addition/aging time (Table 1), since the XRD patterns and FTIR spectra are identical in both cases.

Formation of Co(II) Hydrotalcite-like Phase in Nitrogen. In nitrogen atmosphere, the above metastable pre-hydrotalcite-like structure relaxed rapidly into the Co(II) hydrotalcite-like phase [i.e., α-$Co(OH)_2$] within 5 min. In Figure 3, the XRD pattern of N01 shows hydrotalcite-like features, giving $d_{003} = 8.09$ Å (Table 2) that is close to the reported value ($d_{003} = 7.92$ Å) for α-$Co(OH)_2$.[11] Furthermore, the *d*-values corresponding to successive diffraction by the basal planes agree well with each other, i.e., $d_{003} \approx 2d_{006} \approx 3d_{009}$, following the hydrotalcite-like structure (unit cell with three slabs).[12,13,16] The formed precipitate also shows the typical blue coloration of α-$Co(OH)_2$. Confirmation of this phase (α) can be further obtained from FTIR

(16) Labajos, F. M.; Rives, V. *Inorg. Chem.* **1996**, *35*, 5313.
(17) Drezdzon, M. A. *Inorg. Chem.* **1988**, *27*, 4628.
(18) Fernandez, J. M.; Barriga, C.; Ulibarri, M. A.; Labajos, F. M.; Rives, V. *J. Mater. Chem.* **1994**, *4*, 1117.
(19) Chisem, I. C.; Jones, W. *J. Mater. Chem.* **1994**, *4*, 1737.
(20) Kruissink, E.; van Reijen, L. L.; Ross, J. R. H. *J. Chem. Soc., Faraday Trans.* 1 **1981**, *77*, 649.
(21) Tekaia Ehlsissen, K.; Delahaya-Vidal, A.; Genin, P.; Figlarz, M.; Willmann, P. *J. Mater. Chem.* **1993**, *3*, 883.

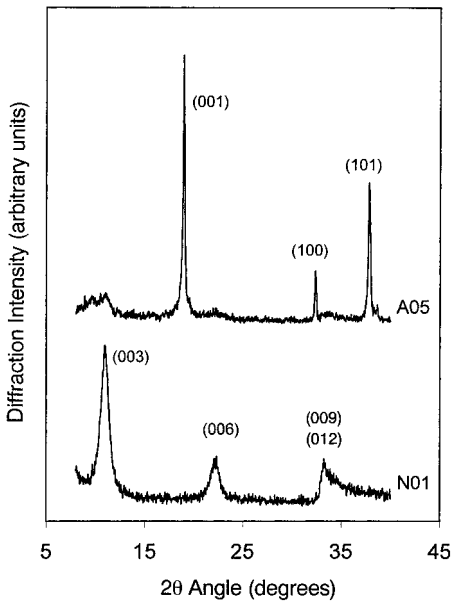

Figure 3. XRD patterns for the Co(II) hydrotalcite-like compound N01 and Co(II) brucite-like compound A05.

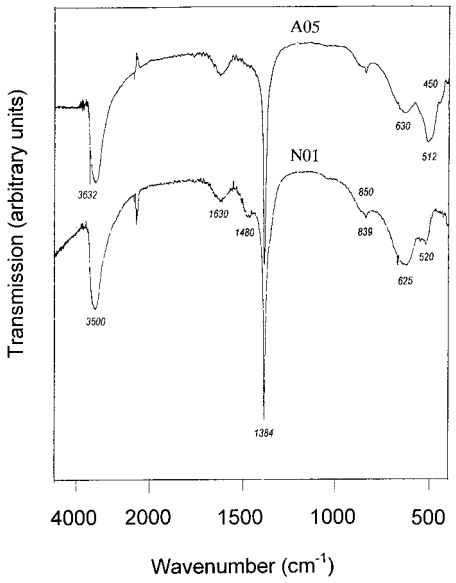

Figure 4. FTIR spectra for the Co(II) hydrotalcite-like compound N01 and Co(II) brucite-like compound A05.

investigations. Shown in Figure 4 for the N01 sample, a large O−H absorption band centered at ca. 3500 cm^{-1} can be assigned to O−H group stretches of gallery water molecules and of H-bound O−H groups in cobalt(II) hydroxide.[18,19,22] Peaks at 1384 and 839 cm^{-1} can be attributed respectively to ν_3 and ν_2 vibrational modes of NO_3^- intercalated in the interlayers.[18−20] The small peak at 1480 cm^{-1} is assigned to monodentate species [symmetric vibration mode: $\nu_s(ONO_2)$, which will discussed together with those in Figure 6]. The peak at 827 cm^{-1} of the N00 and A00 precursors is shifted to 839 cm^{-1} now, indicating a reduction in perturbation of the intercalated NO_3^- compared to that in the pre-HT sample. Absorption bands shown at 850 and 520 cm^{-1} (Table 3) are associated with metal−oxygen vibrations.[12,23]

(22) Kannan, S.; Swamy, C. S. *J. Mater. Sci. Lett.* **1992**, *11*, 1585.
(23) Busca, G.; Trifiro, F.; Vaccari, A. *Langmuir* **1990**, *6*, 1440.

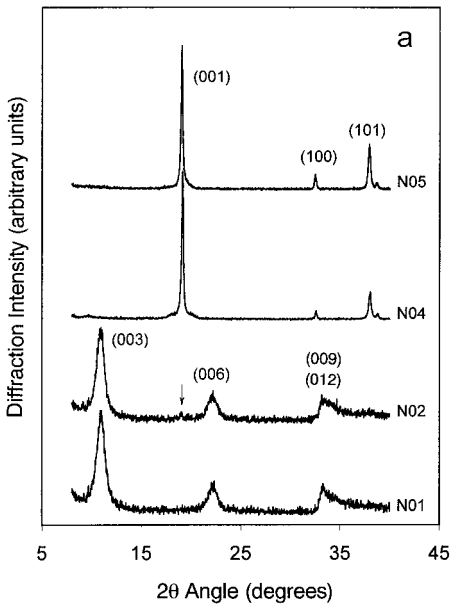

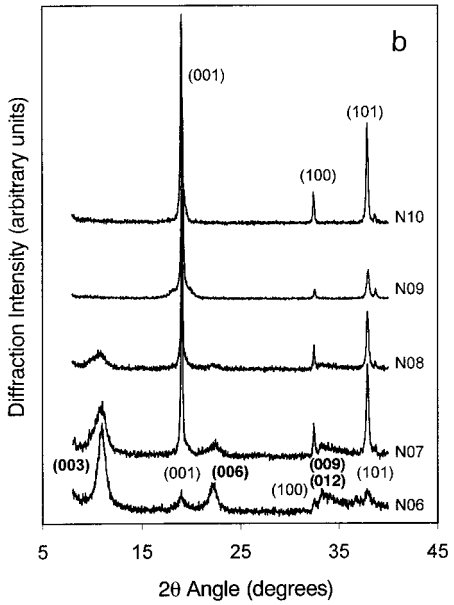

Figure 5. (a) XRD patterns of N01−N05 and (b) XRD patterns of N06−N10 for illustration of the Co(II) hydrotalcite-like phase to Co(II) brucite-like phase transformation in nitrogen.

In view of no oxidant introduced during the precipitation, the oxidation state of cobalt should in principle remain unchanged (+2) in the N01 sample. The redox titration detailed in the Experimental Section indeed indicates that there is no Co^{3+} present in the sample, while anion species are intercalated ($[Co^{3+}]/[Co] = 0$ and $[NO_3^- + 2CO_3^{2-}]/[Co] = 0.18$; Table 4). Taking the current experimental conditions into consideration, among the many existing models, formation of α-$Co(OH)_2$ can be attributed to the existence of hydroxyl vacancies.[2,11] According to this model, some OH^- groups in the N01 sample are missing (or dislocated) from the normal cobalt(II) hydroxide (i.e., β-$Co(OH)_2$ phase). To restore charge balance, anion intercalation occurs during the fast pre-HT structural evolution, which leads to the formation of a Co(II) hydrotalcite-like phase.

The above OH-deficit model was further verified with color changes[1,2,6−8] in these experiments. When the

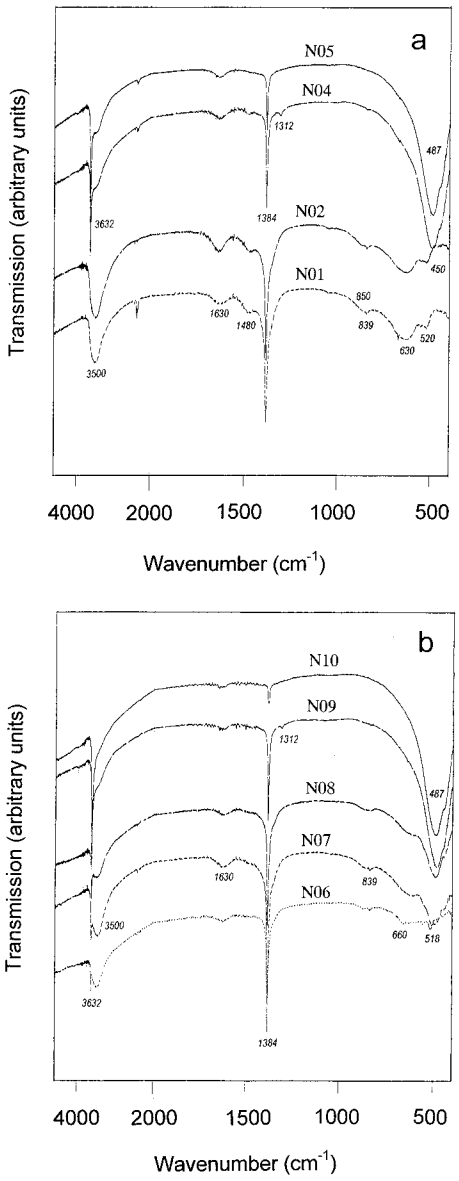

Figure 6. (a) FTIR spectra of N01−N05 and (b) FTIR spectra of N06−N10 for illustration of the Co(II) hydrotalcite-like phase to Co(II) brucite-like phase transformation in nitrogen.

Table 3. Summary of FTIR Characteristic Absorptions for Some Representative Samples with Different Crystallographic Phases

sample	phase[a]	O−H[b]	NO_3^- [b]	M−O[b]
N00, A00	Pre-HT	3500 (s,b) 1620 (m,b)	1480 (w) 1435 (b,w) 1384 (vs) 839 (w) 827 (w)	850 (w,b) 650 (w,b) 520 (w)
N01, N02	HT(II)	3500 (s,b) 1620 (m,b)	1480 (b,w) 1384 (vs) 839 (w)	850 (w,b) 630 (m,b) 520 (w)
N05, N10	B(II)	3632 (s)	1384 (m)	487 (vs,b) 450 (sh)
A11, AN08	HT(II,III)	3500 (s,b) 1620 (m,b)	1384 (vs) 839 (w) 827 (w)	850 (w,b) 630 (w,b) 561 (w) 517 (w)

[a] Phase notation is the same as in Table 2. [b] Intensity is presented by the letters in brackets: s, strong; b, broad; m, medium; vs, very strong; sh, shoulder; w, weak.

weak base ammoniacal solution was replaced with a NaOH solution whose $[OH^-]$ was enhanced, the blue color (α-$Co(OH)_2$) appeared immediately and then changed to pink-red (β-$Co(OH)_2$) under either nitrogen or air atmosphere.

Table 4. Elemental Analysis Results for the Representative Samples

sample	$[Co^{3+}]/[Co]$[a]	$[NO_3^- + 2CO_3^{2-}]/[Co]$[b]	structural phase[c]
N01	0	0.18	HT(II)
N05	0	0.02	B(II)
A05	0.04	0.13	B(II)+HT(II,III)+pre-HT
A06	0.10	0.17	B(II)+HT(II,III)
A07	0.16	0.23	HT(II,III)+B(II)
A08	0.27	0.24	HT(II,III)+B(II)
A09	0.29	0.29	HT(II,III)
A10	0.28	0.32	HT(II,III)
A11	0.27	0.24	HT(II,III)
AN07	0.22	0.21	HT(II,III)

[a] $[Co^{3+}]/[Co]$ is the mole ratio of trivalent cobalt to total cobalt in the precipitate samples. [b] $[NO_3^- + 2CO_3^{2-}]/[Co]$ is the mole ratio of total charges of anion species to total cobalt in the precipitate samples; CO_3^{2-} is at contaminant level (constant trace) due to ambient CO_2 dissolution. [c] Phase notation is the same as in Table 2; order of structural phase appears according to intensity of XRD data.

Formation of Co(II) Brucite-like Phase in Air. Unlike relaxation in nitrogen atmosphere, the metastable pre-hydrotalcite-like phase converts into a brucite-like structure [i.e., β-$Co(OH)_2$] in air. In fact this phase-relaxation occurs rather fast. With 15 min aging, sample A01 shows pronounced diffraction peaks of brucite-type at $2\theta = 19.0°$, 32.4°, and 37.9°, namely (001), (100), and (101).[24] For longer adding/aging times, such as in sample A05, a brucite-like phase has been largely developed; elemental analysis for this phase confirms that no nitrate anions are intercalated. The XRD pattern in Figure 3 indicates a predominant well-crystallized brucite-like phase in this sample (A05). The formation of the brucite-like phase in air is also evidenced by FTIR studies (Figure 4). A new, sharp peak at 3632 cm^{-1}, which is not observed in N01, appears in A05. The peak can be assigned to hydroxyl groups in brucite-like structures due to an increase in basicity, although the interlayer water (O−H, ca. 3500 cm^{-1}) and anions (1384 and 839 cm^{-1}) shown in the pre-HT are still present in this spectrum.[18−20] Absorptions at 400−600 cm^{-1} region can be assigned to metal−oxygen vibrations and metal−oxygen−hydrogen bending vibrations in the brucite-like octahedron sheet,[3,5] which are substantially different from those in the N01.

The actual cause of this early formation of the Co(II) brucite-like phase in air is not clear at the present time. However, its formation must be related to air that contains oxygen, in view of the unique preparative conditions, which will be addressed in later sections.

Co(II) Hydrotalcite-like Phase to Co(II) Brucite-like Phase Conversion in Nitrogen. On the basis of XRD results, the conversion of the Co(II) hydrotalcite-like phase to the Co(II) brucite-like phase is clearly demonstrated in Figure 5a. In the sample series N01−N05, the addition time was fixed at 15 s while the aging time was varied (Table 1). The interlayer spacing d_{001} obtained from the sample N05 (4.66 Å, Table 2) is similar to that of β-$Co(OH)_2$ reported in the literature

(24) Powder Diffraction File, Card No. 45-0031. Joint Committee on Powder Diffraction Standards, Swarthmore, PA, 1995.

(4.664 Å).[24] Starting from sample N02, a small peak [(001) of the brucite-like phase, indicated by an arrow] emerges after 2 h of aging. The initial Co(II) hydrotalcite-like phase has been completely transformed into the Co(II) brucite-like phase, as shown in N04 for 6 h aging (Table 1). The Co(II) brucite-like phase was also confirmed with the EA method; there are virtually no Co^{3+} and interlayer anions (N05, Table 4). To illustrate this phase transformation in detail, XRD patterns for N06−N10 are displayed in Figure 5b. In the preparation of these samples, the addition time of the cobalt cation solution was changed while the aging time was fixed at 2 h (a time sufficient for emergence of the Co(II) brucite-like phase, e.g., similar to the N02 case). As can be seen, a complete formation of a Co(II) brucite-like phase had been achieved in sample N09 after only a total of 2.5 h of addition and aging. Thus, compared with N01−N05, slow addition technique utilized in N06−N10 can shorten the time required for the Co(II) hydrotalcite-like to brucite-like phase conversion. Apparently the OH^--deficit model in formation of α-$Co(OH)_2$ can explain why slow addition results in fast conversion to β-$Co(OH)_2$, since better crytallinity and fewer OH^- defects are generally expected in a slower process.

The color changes of these samples also reflect the above transformation. From N01 to N05 and from N06 to N10, the blue of α-$Co(OH)_2$ is sequentially changed to gray and then to pink-red, a typical color for the Co(II) brucite-like phase.[1,2,6−8] This phase conversion can also be noted from the FTIR investigations reported in Figure 6a. Three significant changes in IR spectra can be observed. Around 3500 cm^{-1}, the broad peak attributed to O−H groups of intercalated water and hydrogen-bound O−H groups of hydroxide becomes weaker and weaker as aging time increases. Simultaneously, a sharp peak at 3632 cm^{-1} attributed to O−H stretching vibrations of brucite-like phases emerges in N02 as a small shoulder and becomes stronger in N04 and N05.[22,25,26] On the contrary, the intensities of the peaks at 1384 and 839 cm^{-1} due to intercalated NO_3^- decrease gradually. The small peak at 1480 cm^{-1} can be assigned to monodentate nitrate species [symmetric vibration mode, $\nu_s(ONO_2)$].[27,28] The tiny peak at 1312 cm^{-1} can be observed in the N04 (and similarly in N09) sample when the amount of NO_3^- is significantly reduced. This peak is normally assigned to asymmetric vibrations of monodentate nitrate [$\nu_{as}(ONO_2)$].[27,28] Below 1000 cm^{-1}, several peaks mainly from metal−oxygen (M−O) vibrations become one large broad band at 487 cm^{-1}, which indicates a change of M−O vibration modes from hydrotalcite-like to brucite-like phase, as discussed for the A05 sample. Similar observations can also made in Figure 6b for samples N06−N10. As discussed, the intensification of the sharp peak at 3632 cm^{-1} and the broad band at 487−490 cm^{-1} is accompanied by the weakening of the broad peak at 3500 cm^{-1} and the sharp one at 1384 cm^{-1}, when addition time was extended.

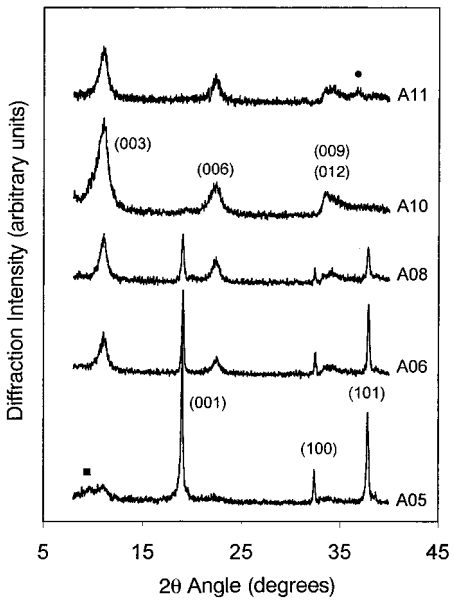

Figure 7. XRD patterns of A05−A11 for illustration of the Co(II) brucite-like phase to Co(II,III) hydrotalcite-like phase transformation in air; pre-HT phase is marked with ■ and Co_3O_4 phase with ●.

It should be mentioned that the IR spectra of Co(II) HT precipitates are very similar to that reported for α-$Co(OH)_2$.[11] Although the weak vibration at 1480 cm^{-1} indicates some lowering of nitrate ion symmetry, the D_{3h} related vibrations (1384 and 839 cm^{-1}) are predominant in these samples. Therefore, formation of basic salts of Co(II) such as $Co_5(OH)_8(NO_3)_2$ and $Co_2(OH)_3NO_3$ can be ruled out, because the 1480 cm^{-1} absorption is too weak and most of IR peaks known for cobalt hydroxide nitrites are not detected.[28]

Co(II) Brucite-like Phase to Co(II,III) Hydrotalcite-like Phase Conversion in Air. As mentioned earlier, samples A01−A04 show characteristics of brucite-like phases. However, the (001) line of the pre-hydrotalcite-like phase persists, although the intensity has been greatly reduced in the sequence from A00 to A04. This prephase can still be traced in sample A05, despite a predominant brucite-like phase. Unlike trends shown in N01−N05 and N06−N10, samples A05−A11 reported in Figure 7 show a reversed phase transformation, i.e., a transition from a brucite-like to a hydrotalcite-like phase. The interlayer spacing for this HT phase is $d_{003} = 7.98$ Å (Table 2; the same value is obtained for samples AN05−AN08 in the next section). Since air contains oxygen, certain redox reactions might be involved in this phase change. For example, in the presence of oxidant O_2, $Co^{2+}(3d^7)$ may lose one electron, becoming $Co^{3+}(3d^6)$. The oxidation of Co^{2+} with air/oxygen in fact has been found in our recent investigations on Mg−Co oxides and layered double-hydroxides of $Mg_{0.3}Co^{(II)}_{0.6}Co^{(III)}_{0.2}(OH)_2(NO_3)_{0.2}\cdot H_2O$.[29,30] Indeed, the formation of $Co^{3+}(3d^6)$ cations with air has also been found for the A05−A11 series. As reported in Table 4, the Co^{3+} content increases with air-aging time, which is balanced nicely by anion species when the brucite-like phase is fully converted (A09−A11). Therefore, samples A09−A11 can be assigned unambiguously to

(25) Grey, I. E.; Ragozzini, R. *J. Solid State Chem.* **1991**, *94*, 244.
(26) Ulibarri, M. A.; Hernandez, M. J.; Cornejo, J. *J. Mater. Sci.* **1991**, *26*, 1512.
(27) Schraml-Marth, M.; Wokaun, A.; Baiker, A. *J. Catal.* **1992**, *138*, 306.
(28) Zotov, N.; Petrov, K.; Dimitrova-Pankova, M. *J. Phys. Chem. Solids* **1990**, *51*, 1199.
(29) Qian, M.; Zeng, H. C. *J. Mater. Chem.* **1997**, *7*, 493.
(30) Zeng, H. C.; Xu, Z. P.; Qian, M. *Chem. Mater.* **1998**, *10*, 2277.

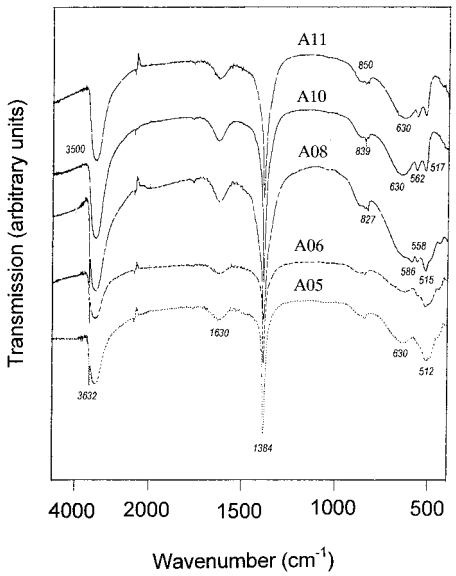

Figure 8. FTIR spectra of A05−A11 for illustration of the Co(II) brucite-like phase to Co(II,III) hydrotalcite-like phase transformation in air.

Co(II,III) hydrotalcite-like compounds, which validates the mixed valent state model initially proposed for nickel hydroxides. [6]

Using a constant addition time of 4 min, the total conversion to the Co(II,III) hydrotalcite-like phase occurs after 24 h of aging (i.e., A10). However, using a longer addition time, such as in the samples A12-A15, the above phase transformation can also be completed at a much faster rate. For example, in the case of A15, the brucite-like phase has been significantly eliminated using an addition time of 42 min and an aging time of 2 h. Therefore, addition time plays a more important role than aging time in the phase conversion.

Under the current experimental conditions, when a prolonged aging in air is carried out, the crystallinity of precipitate may be reduced. In fact, a small diffraction peak of the Co_3O_4 phase becomes noticeable in sample A11,[31] which can be attributed to overoxidation of Co(II) brucite-like compounds. The presence of trace Co_3O_4 was also observed in other experiments that had long aging time in air. In accordance with XRD and EA analyses, oxidation of $Co^{2+}(3d^7)$ with air/oxygen is observed. Hence, to obtain the Co(II,III) hydrotalcite-type samples with higher crystallinity, one should optimize aging time.

The above phase change is also reflected in FTIR spectra measured for the A01−A15 series. Figure 8 gives some representative spectra (A05−A11) with respect to their XRD patterns in Figure 7. A gradual disappearance of the sharp peak at 3632 cm^{-1} indicates a continuous diminution of the brucite-like phase during the above phase transformation. Before complete transformation (A08), IR peaks for ν_3 and ν_2 vibrational modes of NO_3^- become more pronounced. In particular, the peak at 827 cm^{-1} is more intense than that at 839 cm^{-1} in the spectrum of A08.[18−20] In A10 (and similarly in A15) three new peaks for the hydrotalcite-like phase M−O are found at 630, 562, and 517 cm^{-1}, respectively, while that at 512 cm^{-1} for the brucite-like A05 sample is no longer observable.[12,23]

The difference in FTIR spectra between Co(II) and Co(II,III) hydrotalcite-like phase is substantial. For Co(II) HT-like samples (e.g., N01 in Figure 4), there is an extra peak at 1480 cm^{-1}, which indicates a lowering of NO_3^- symmetry in the samples. Since the 1480 cm^{-1} vibration is normally assigned to NO_3^- in C_{2v} symmetry,[18−20] it is deduced that the NO_3^- anion is perturbed more severely in the Co(II) HT-like compound. The cause may be attributed to more direct interaction of the anion with Co^{2+} cations. In the Co(II,III) HT-like phase (e.g., A05 in Figure 4 and A10−A11 in Figure 8), on the other hand, NO_3^- anion is located in a planar position since the 1384 cm^{-1} peak remains relatively unperturbed (i.e. NO_3^- anion with D_{3h} symmetry in the interlayer space).[18−20] In the Co−O stretching region, new peaks at 558−562 cm^{-1} are exclusively observed only in air-aged HT-like samples (A06−A11).

Conversions in Combined Preparative Atmospheres. For samples NA01−NA16 and AN01−AN08, two different preparative gases were used for aging (Table 1). Experiments were done, switching from nitrogen to air or from air to nitrogen, to differentiate the role each gas was playing in phase transformation. Only XRD/FTIR results of these experiments are reported, since results are similar to those analyzed in previous sections.

For example, preparation conditions for samples NA01−NA05 were quite similar to those of N06−N10, except that the aging was primarily conducted in air (Table 1). On the basis of XRD/FTIR investigations, structural evolution in NA01−NA05 is essentially similar to N06−N10 samples shown in Figures 5b and 6b. Apparently, conversion from Co(II) hydrotalcite-like phase to brucite-like phase is largely complete during addition in nitrogen. The change of aging atmosphere to air shows no noticeable influence on this phase transformation.

As shown earlier in samples N01−N05 and N06−N10, the Co(II) hydrotalcite-like phase to Co(II) brucite-like phase conversion occurs in nitrogen atmosphere (Figures 5 and 6). Instead of nitrogen, nonetheless, it would be of interest to explore whether the above transformation can take place in air or not. Since samples N06 and N07 contain both Co(II) hydrotalcite-like and Co(II) brucite-like phases (Figures 5b and 6b), similar preparative conditions were employed in samples NA06−NA13 to form initial Co(II) hydrotalcite-like phases (Table 1). With prolonged aging in air (0−96 h), the hydrotalcite-like phases remain (XRD/FTIR analysis). Therefore it is concluded that the as-prepared Co(II) hydrotalcite-like phase cannot be converted into Co(II) brucite-like phase in air. Instead, this divalent HT-like phase has been changed to a Co(II,III) hydrotalcite-like phase in the NA06−NA13 series due to oxidation in air.

The chemical convertibility of the Co(II) brucite-like phase to HT-phase was examined in samples NA14−NA16 (Table 1). Prolonged aging in nitrogen (20 h) ensured good crystallinity of Co(II) brucite-like phases [see also N01−N05 and N06−N10 samples (Figures 5 and 6)]. An even longer aging time (up to 96 h) was used to try to convert this nitrogen-aged Co(II) brucite-like phase to Co(II,III) hydrotalcite-type compounds. XRD/

(31) Powder Diffraction File, Card No. 9-418. Joint Committee on Powder Diffraction Standards, Swarthmore, PA, 1967.

FTIR results of all three samples show no sign of the hydrotalcite-like phase. Therefore, it is evident that a well-crystallized Co(II) brucite-like phase cannot be transformed into a hydrotalcite-like phase, regardless of type of atmosphere utilized under these conditions.

The newly formed Co(II) brucite-like phase found in A01−A04 and A05 can be converted into the Co(II,III) hydrotalcite-like phase (Figure 7) in air atmosphere. However, the brucite-like phase formed in air is always accompanied by a trace of pre-hydrotalcite-like and Co(II,III) hydrotalcite-like phases in these samples. As shown in Figure 7, pre-hydrotalcite-like (001) peaks (unit cell with one slab) and (003) peaks [and probably (006) and (009) peaks] of Co(II,III) hydrotalcite-like phase are visible in the A05 sample. The presence of three phases in A05 may suggest a defective brucite-like β-$Co(OH)_2$ phase which would ease oxidation to the Co(II,III) hydrotalcite-like phase.

Experiments AN01−AN04 were designed to switch off the above oxidative conversion by introducing inert nitrogen (protective gas) to the aged samples (up to 48 h in nitrogen). As expected, based on XRD/FTIR analysis, all samples show no further oxidative conversion to the hydrotalcite-like phase but to a more crystalline Co(II) brucite-like phase in nitrogen.

As evidenced in the N01−N05 and N06−N10 series, the newly formed Co(II) hydrotalcite-like phase can convert into a Co(II) brucite-like phase. However, if the resultant hydrotalcite-like phase of A10−A11 (Figure 7) was similar to that formed in N01, aging in nitrogen should be able to convert it into the Co(II) brucite-like phase, as in the N01−N05 and N06−N10 series (Figure 5). Therefore, comparative experiments of AN05−AN08 were carried out to further probe the formation of the Co(II,III) hydrotalcite-like phase. As indicated by XRD/FTIR analysis, it is not possible to transform these hydrotalcite-like samples into Co(II) brucite-like forms under these experimental conditions, even with a prolonged aging of 72 h in nitrogen (AN08). These results are in accord with the oxidative formation of the Co(II,III) hydrotalcite-like phase. Thus, this new hydrotalcite-like phase is different from the Co(II) hydrotalcite-like phase (α-phase) formed in nitrogen.

On the basis of the above experimental results, an interconversion chart for the brucite-like and hydrotalcite-like phases in cobalt hydroxide compounds is summarized in Figure 9. These interconversions depend heavily on the chemical composition of the atmosphere, the addition time of the cation, and the aging time of the precipitates. In fact, these preparative parameters are closely correlated, as evidenced in the above sections. By selecting the right set of parameters, a cobalt hydroxide with a desired crystallographic structure and appropriate oxidation states for the cobalt cations can be prepared.

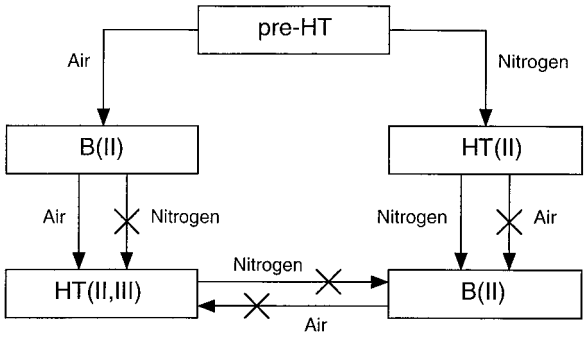

Figure 9. Interconversion chart of the brucite-like and hydrotalcite-like phases in cobalt hydroxide compounds and their preparation conditions.

Conclusions

In summary, a systematic investigation of preparative parameters of cobalt hydroxide synthesis has been carried out. Using different atmospheres, cobalt hydroxides with a desired crystallographic phase can be selectively prepared. A common new precursor compound exists prior to the formations of α- and β-$Co(OH)_2$. The α-$Co(OH)_2$, which is hydrotalcite-like, can be prepared in nitrogen with short-aging times, while brucite-like β-$Co(OH)_2$ can be formed in air with short aging times. The metal in the α-phase is divalent, and α-$Co(OH)_2$ can be converted to β-$Co(OH)_2$ with prolonged aging in nitrogen. An air-prepared β-$Co(OH)_2$, on the other hand, can be transformed into a new hydrotalcite-like phase in which both Co^{2+} and Co^{3+} are present. On the basis of these findings, interconversions between brucite-like and hydrotalcite-like phases of cobalt hydroxides can be controlled explicitly under various preparative conditions. Among the three preparative parameters, atmosphere is the most important one in controlling phase transformations, while addition time of cation is more important than aging time.

CM980420B